The EMBO Journal (2004) 23, 1040–1050 | © 2004 European Molecular Biology Organization | All Rights Reserved 0261-4189/04
www.embojournal.org

THE EMBO JOURNAL

Tyrosine phosphorylation of GluR2 is required for insulin-stimulated AMPA receptor endocytosis and LTD

Gholamreza Ahmadian[1], William Ju[2,4], Lidong Liu[2,4], Michael Wyszynski[3], Sang Hyoung Lee[3], Anthone W Dunah[3], Changiz Taghibiglou[4], Yushan Wang[4], Jie Lu[4], Tak Pan Wong[4], Morgan Sheng[3] and Yu Tian Wang[2,4,*]

[1]National Research Center for Genetic Engineering and Biotechnology, Tehran, Iran, [2]Programme in Brain and Behaviour, Hospital for Sick Children and Department of Laboratory Medicine & Pathobiology, University of Toronto, Toronto, Canada, [3]Center for Learning and Memory and Howard Hughes Medical Institute, Massachusetts Institute of Technology, Cambridge, MA, USA and [4]Department of Medicine & Brain Research Centre, Vancouver Hospital & Health Sciences Centre, University of British Columbia, Vancouver, Canada

The α-amino-3-hydroxy-5-methylisoxazole-4-propionic acid (AMPA) subtype of glutamate receptors is subject to functionally distinct constitutive and regulated clathrin-dependent endocytosis, contributing to various forms of synaptic plasticity. In HEK293 cells transiently expressing GluR1 or GluR2 mutants containing domain deletions or point mutations in their intracellular carboxyl termini (CT), we found that deletion of the first 10 amino acids (834–843) selectively reduced the rate of constitutive AMPA receptor endocytosis, whereas truncation of the last 15 amino acids of the GluR2 CT, or point mutation of the tyrosine residues in this region, only eliminated the regulated (insulin-stimulated) endocytosis. Moreover, in hippocampal slices, both insulin treatment and low-frequency stimulation (LFS) specifically stimulated tyrosine phosphorylation of the GluR2 subunits of native AMPA receptors, and the enhanced phosphorylation appears necessary for both insulin- and LFS-induced long-term depression of AMPA receptor-mediated excitatory postsynaptic currents. Thus, our results demonstrate that constitutive and regulated AMPA receptor endocytosis requires different sequences within GluR CTs and tyrosine phosphorylation of GluR2 CT is required for the regulated AMPA receptor endocytosis and hence the expression of certain forms of synaptic plasticity.

The EMBO Journal (2004) **23,** 1040–1050. doi:10.1038/sj.emboj.7600126; Published online 19 February 2004
Subject Categories: membranes & transport; neuroscience
Keywords: AMPA receptor; endocytosis; hippocampal slices; LTP; tyrosine phosphorylation

*Corresponding author. Department of Medicine & Brain Research Centre, Vancouver Hospital & Health Sciences Centre, University of British Columbia, 2211 Wesbrook Mall, Vancouver, BC, Canada V6T 2B5. Tel.: +1 604 822 0398; Fax: +1 604 822 7299;
E-mail: ytwang@interchange.ubc.ca

Received: 25 July 2003; accepted: 23 January 2004; published online: 19 February 2004

Introduction

The α-amino-3-hydroxy-5-methylisoxazole-4-propionic acid (AMPA) subtype of glutamate receptors mediates fast synaptic transmission at the vast majority of excitatory synapses in the mammalian central nervous system. Regulation of AMPA receptor-mediated synaptic transmission is therefore fundamental to both brain functions and dysfunctions. Recent studies have suggested that AMPA receptors undergo cycling between intracellular compartments and the plasma membrane via vesicle-mediated plasma membrane insertion (exocytosis) and internalization (endocytosis) (Man *et al*, 2000a). Regulating these processes can lead to rapid changes in the number of AMPA receptors expressed in the postsynaptic membrane, and thereby contribute to the expression of certain forms of well-characterized synaptic plasticity, including hippocampal long-term potentiation (LTP) (Hayashi *et al*, 2000; Lu *et al*, 2001; Pickard *et al*, 2001) and long-term depression (LTD) (Luscher *et al*, 1999; Luthi *et al*, 1999; Man *et al*, 2000b), as well as cerebellar LTD (Wang and Linden, 2000).

While the mechanisms involved in vesicle-mediated AMPA receptor exocytosis remain elusive, accumulating evidence strongly suggests that AMPA receptor internalization is mediated by clathrin-dependent endocytosis (Carroll *et al*, 1999; Luscher *et al*, 1999; Beattie *et al*, 2000; Lin *et al*, 2000; Man *et al*, 2000b). Furthermore, two distinct types of clathrin-dependent AMPA receptor endocytosis, constitutive and regulated (stimulated), can be classified according to their underlying mechanisms and functional significances. Interfering with the constitutive pathway did not lead to detectable alterations in the number of AMPA receptors on the cell surface (Man *et al*, 2000b), likely because of the existence of a constitutive AMPA receptor exocytosis pathway that counteracts the constitutive endocytosis (Man *et al*, 2000b; Liang and Huganir, 2001). However, stimulating the regulated pathway with insulin or *N*-methyl-D-aspartate (NMDA) leads to a rapid reduction in the number of postsynaptic AMPA receptors and a long-lasting depression of the receptor-mediated synaptic transmission (Beattie *et al*, 2000; Man *et al*, 2000b; Wang and Linden, 2000).

The molecular mechanisms mediating the constitutive and regulated AMPA receptor endocytotic pathways remain largely unknown. Native AMPA receptors are currently thought to be heteromeric protein complexes assembled from combinations of GluR subunits 1–4 (Hollmann and Heinemann, 1994). The exact subunit composition of most native AMPA receptors remains unknown, but it has been suggested that native AMPA receptors in rat hippocampus largely contain either GluR1/2 or GluR2/3 subunits (Wenthold *et al*, 1996). When transiently expressed in non-neuronal mammalian cells, individual GluR subunits can form functional homomeric AMPA receptor channels, and most importantly AMPA receptors in these heterologous expression systems can

undergo both constitutive and regulated clathrin-dependent endocytosis (Lin *et al*, 2000; Man *et al*, 2000b). In HEK293 cells, transiently expressed GluR1 and GluR2 homomeric AMPA receptors undergo constitutive endocytosis at similar rates. It is therefore likely that the constitutive pathway is common to all GluR subunits. In contrast, the insulin-stimulated (regulated) endocytotic pathway is GluR2 subunit specific and dependent upon unique sequences present in the carboxyl termini (CT) (Man *et al*, 2000b). Consistent with the importance of the GluR2 CT in regulated endocytosis, several recent studies have strongly implicated a role for the PDZ-binding domain of the GluR2 CT ($-S_{880}$VKI), which is known to interact with several PDZ-containing proteins, in the regulated AMPA receptor internalization (Chung *et al*, 2000), and hence in the expression of both hippocampal (Kim *et al*, 2001) and cerebellar LTD (Matsuda *et al*, 2000; Xia *et al*, 2000). However, in HEK293 cells transiently expressing recombinant GluR2 homomeric AMPA receptors, deleting the GluR2 CT PDZ-binding motif did not notably affect insulin-induced receptor endocytosis (Lin *et al*, 2000), suggesting that there may be some other region(s) within the GluR2 CT, in addition to the PDZ domain, that is also required for GluR2-dependent regulated AMPA receptor endocytosis. In the present study, we further investigated this possibility by employing systematic domain deletions of the GluR2 CT, coupled with site-directed point mutations within this region.

Results

Distinct sequences within the GluR2 CT are required for constitutive and regulated AMPA receptor endocytosis

To identify sequence determinants for constitutive and insulin-stimulated AMPA receptor endocytosis, we made six GluR2 mutants containing various deletions of the GluR2 CT (Figure 1). All constructs, except GluR2$_{\Delta 854}$, were HA tagged in the extracellular amino-terminal region. Following transient transfection into HEK293 cells, these constructs were expressed at a level comparable to their wild-type counterparts, HA–GluR2 or GluR2, as determined by a colorimetric cell-ELISA assay under permeabilized cell conditions (Figure 1C). The ability of these mutants to undergo both constitutive and regulated endocytosis was assayed as described previously (Man *et al*, 2000b). Surface receptors in live cells were prelabelled with an anti-HA antibody (or an antibody against the extracellular N-terminal domain of GluR2 in the case of GluR2$_{\Delta 854}$) at 4°C (which blocks endocytosis). Surface labelled cells were then incubated at 37°C for 30 min to allow endocytosis to resume both in the absence and presence of insulin (0.5 μM) to determine changes in constitutive (basal) and regulated (insulin-stimulated) AMPA receptor endocytosis, respectively (Figure 2). Internalized receptors were visualized by confocal microscopy and quantitated by colorimetric cell-ELISA-based receptor

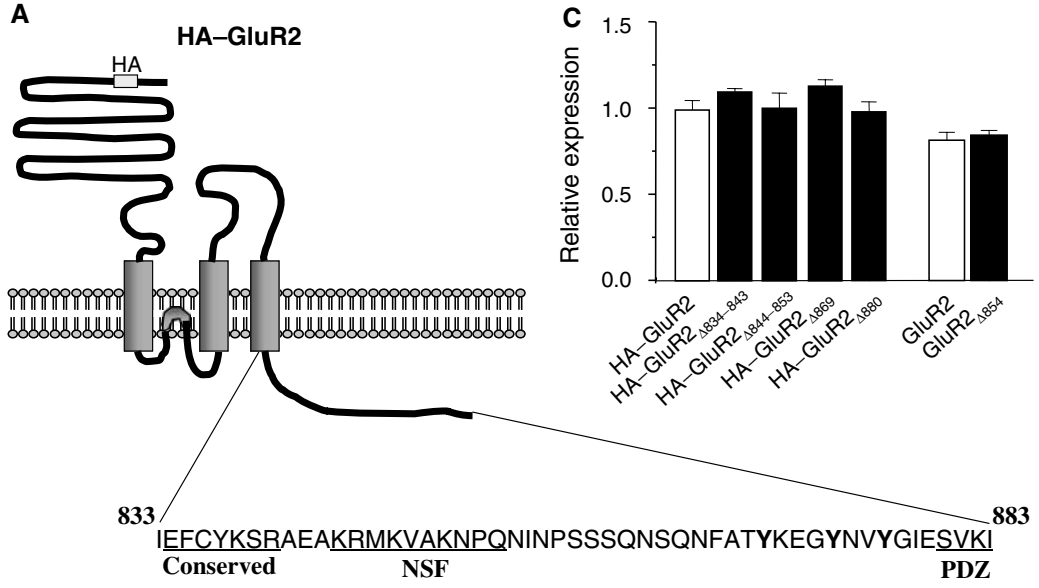

B

HA–GluR2$_{\Delta 834–843}$	I----------KRMKVAKNPQNINPSSSQNSQNFATYKEGYNVYGIESVKI
HA–GluR2$_{\Delta 844–853}$	IEFCYKSRAEA----------NINPSSSQNSQNFATYKEGYNVYGIESVKI
GluR2$_{\Delta 854}$	IEFCYKSRAEAKRMKVAKNPQ
HA–GluR2$_{\Delta 869}$	IEFCYKSRAEAKRMKVAKNPQNINPSSSQNSQNFAT
HA–GluR2$_{\Delta 880}$	IEFCYKSRAEAKRMKVAKNPQNINPSSSQNSQNFATYKEGYNVYGIE

Figure 1 Construction of GluR2 internal deletion or CT truncation mutants. (**A**) Putative topology of AMPA receptor GluR2 subunit with HA tag inserted in the N-terminal extracellular domain. The expanded region shows the amino-acid sequence of the CT of GluR2. Sequences conserved among GluR1–4 (conserved) and those involved in its interaction with NSF (NSF) or PDZ domain-containing proteins (PDZ) are underlined. (**B**) CT sequences of internal deletion or truncation mutants of the full-length HA-tagged or nontagged GluR2 subunit. (**C**) Expression levels of the constructs following transient transfection into HEK293 cells were determined by cell-ELISA assays using an anti-HA antibody for HA-tagged constructs, or an anti-GluR2 subunit antibody for the non-HA-tagged construct, under permeabilized conditions. The level of expression was normalized to the expression level of HA–GluR2.

internalization assays (Figures 2A and B). In order to determine whether changes in internalization produced by these mutations were able to alter surface receptor numbers, we also measured the steady-state level of cell-surface AMPA receptors using colorimetric cell-ELISA-based cell-surface receptor assays (Figure 2C) (Man *et al*, 2000b). As shown in Figures 2A and B, and consistent with our previous report, wild-type GluR2 receptors underwent both constitutive and insulin-stimulated endocytosis. Thus, in the absence of insulin, approximately 25% of the cell-surface receptors were endocytosed within 30 min and this proportion was increased to 48% following brief insulin stimulation (0.5 μM, 10 min). This facilitated endocytosis was associated with a significant reduction in the level of AMPA receptors expressed on the cell surface (Figure 2C). Truncation of the last four amino acids ($GluR2_{\Delta 880}$), which form the PDZ-binding motif, did not have any observable effects on either constitutive or regulated endocytosis. However, truncation of the last 30 ($GluR2_{\Delta 854}$) or 15 residues ($GluR2_{\Delta 869}$) completely abolished the insulin-induced AMPA receptor endocytosis, and the reduction in its cell-surface expression (Figures 2A–C). Interestingly, neither truncation altered the degree of constitutive AMPA receptor endocytosis (Figure 2B) or the basal level of receptor expression on the cell surface (Figure 2C). These results suggest that the 11 amino acids immediately preceding the PDZ-binding domain in the GluR2 CT may contain a critical signal required for the regulated endocytosis.

Deletion of the first 10 amino acids of the GluR2 CT, on the other hand, resulted in a significant decrease in the rate of constitutive internalization of $GluR2_{\Delta 834-843}$ (Figures 2A and B). However, this internal deletion did not alter the steady-state level of cell-surface AMPA receptor expression (Figure 2C). Nor did it alter the responsiveness to insulin, as $GluR2_{\Delta 834-843}$ showed enhanced internalization similar in magnitude to wild-type GluR2 (Figures 2B and C). As the first seven residues of the 10 amino acids deleted are conserved among GluR1–4, these results correspond well with our previous results that both GluR1 and GluR2 undergo constitutive endocytosis at a similar rate (Man *et al*, 2000b). In contrast, the internal deletion mutant $GluR2_{\Delta 844-853}$ showed no significant change in the degree of constitutive endocytosis (Figure 2B), but exhibited a small, insignificant decrease in insulin-stimulated endocytosis (Figure 2B) and a reduction in the steady-state receptor level on the cell surface (Figure 2C). As the 10 amino-acid residues deleted from this mutant contained the NSF- and AP2-binding domains, these results are consistent with the previously suspected role of NSF binding in AMPA receptor insertion into and/or stabilization in the plasma membrane (Lee *et al*, 2002; Duprat *et al*, 2003).

GluR2 CT tyrosine phosphorylation is required for insulin-stimulated AMPA receptor endocytosis

As the 11-amino-acid stretch required for insulin-stimulated endocytosis contains three tyrosine residues, we next examined whether the tyrosine residues are substrates of certain tyrosine kinases. We performed *in vitro* kinase assays using active recombinant Src and glutathione *S*-transferase (GST) fusion proteins of the carboxyl tails of GluR1 (GST–GluR1CT) and GluR2 (GST–GluR2CT) (Figure 3A). GST–GluR2CT, but not GST–GluR1CT or GST alone, is specifically phosphorylated by Src kinase. Moreover, we found that the recombinant

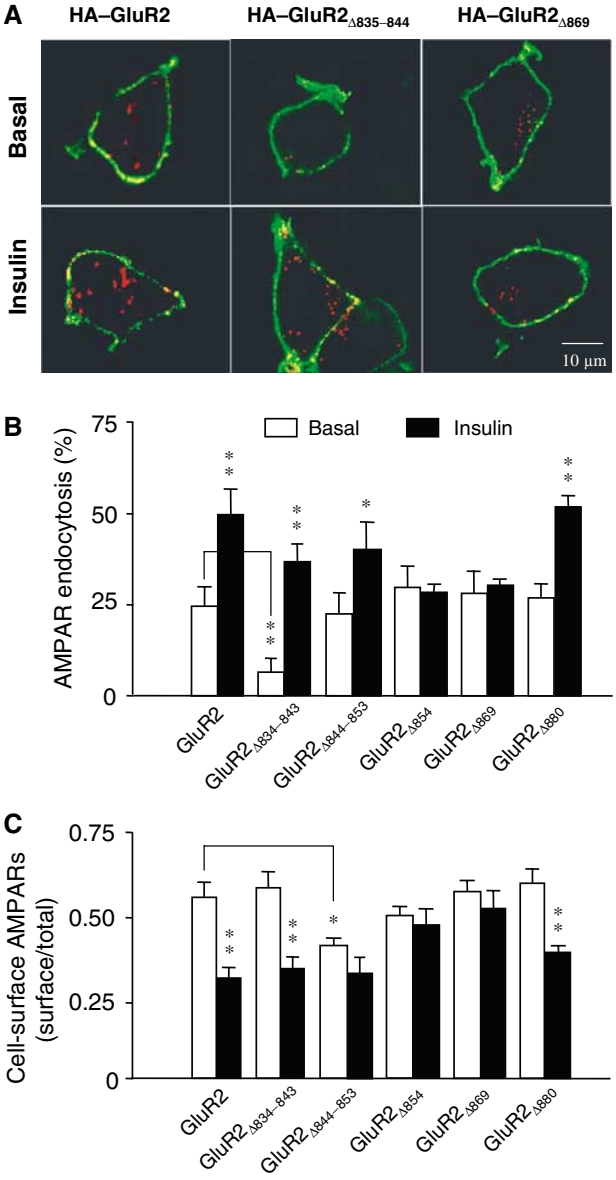

Figure 2 Effects of GluR2 CT mutations on endocytosis and cell-surface expression of AMPA receptors. (**A**) Representative confocal images of HEK293 cells transiently transfected with HA-tagged GluR2 or GluR2 mutants (as indicated). Transfected cells were prelabeled with anti-HA antibody and then receptor endocytosis was evaluated under basal conditions (constitutive endocytosis) or following insulin stimulation (0.5 μM, 10 min; regulated endocytosis). Cell-surface receptors were stained with FITC (green) under nonpermeant conditions and internalized receptors were subsequently stained with Cy3 (red) after cell permeabilization. (**B**) Quantitation of the changes in constitutive (basal) and regulated (insulin) endocytosis of GluR2 and its various mutants using a colorimetric ELISA assay with prelabeled cells following the internalization of the receptors over 30 min (% AMPAR endocytosis = 100% − remaining cell-surface receptors/total number of receptors; $n = 6$). Control: internalization measured in cells at 4°C without any 37°C exposure. (**C**) Cell-surface AMPA receptors in HEK293 cells transiently expressing GluR2 and its various mutants were quantitated using colorimetric cell-ELISA-based cell-surface receptor assays ($n = 6$). Statistical comparisons were made between basal and insulin-treated conditions, except where indicated by lines. $^{*}P < 0.05$, $^{**}P < 0.01$.

Src kinase phosphorylated a GST fusion protein containing the nine-amino-acid stretch including all three GluR2-unique tyrosine residues (GST–Y_{869}KEGY_{873}NVY_{876}G) and this

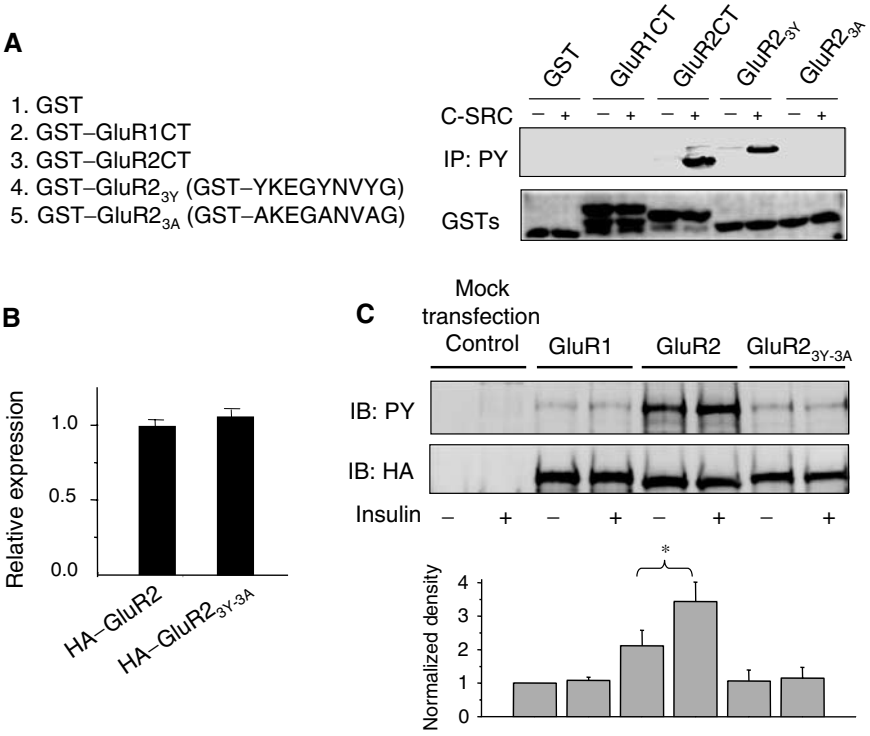

Figure 3 Insulin increases phosphorylation of tyrosine residues within the GluR2 CT region. (**A**) *In vitro* tyrosine phosphorylation of the GluR2 CT. GST fusion proteins of the GluR1 CT (GST–GluR1CT), the GluR2 CT (GST–GluR2CT), residues 869–876 (YKEGYNVYG) of the GluR2 CT (GST–GluR2$_{3Y}$) and the same amino-acid stretch of the GluR2 CT with its tyrosine residues replaced by alanines (GST–GluR2$_{3A}$), along with GST as control, were incubated in the absence (−) or presence (+) of active recombinant pp60 c-Src. Phosphorylation products were immunoblotted using an antiphosphotyrosine antibody (top panel). Ponceau S staining of the same blot showed that a similar amount of GST fusion protein was used in each of the reactions (lower panel). (**B**) Expression levels of HA–GluR2 and HA–GluR2$_{3Y-3A}$ (where tyrosines 869, 873 and 876 were mutated to alanines) 48 h after transient transfection into HEK293 cells were determined by a cell-ELISA assay using permeabilized cells. (**C**) HEK293 cells transiently transfected with HA–GluR1, HA–GluR2 or HA–GluR2$_{3Y-3A}$, along with empty vector (mock transfection) as control. After 48 h, the cells were treated with or without 0.5 μM insulin for 10 min. The lysates were then subjected to immunoprecipitation with an anti-HA antibody under denaturing conditions and immunoblotting with an antiphosphotyrosine antibody (top blot; IB: PY). The same blot was stripped and re-immunoblotted with the anti-HA antibody to ensure similar immunoprecipitation efficiency in all individual experiments (lower blot; IB: HA). The bar graph at the bottom summarizes data from five individual experiments. Values are normalized to GluR1 without insulin treatment. $^*P<0.05$.

phosphorylation was abolished by mutating these tyrosine residues into alanines (GST–A$_{869}$KEGA$_{873}$NVA$_{876}$G).

To determine whether these GluR2 CT tyrosine residues are phosphorylated *in situ* by endogenous tyrosine kinase activity in response to insulin stimulation, we generated a GluR2 subunit mutant in which tyrosine residues Y869, Y873 and Y876 were mutated into alanines (HA–GluR2$_{3Y-3A}$). When transiently expressed in HEK293 cells, the mutant was expressed at the same level as its wild-type GluR2 counterpart (Figure 3B). We first examined the potential phosphorylation of these tyrosine residues *in situ* in cells transiently expressing HA–GluR2, HA–GluR2$_{3Y-3A}$ or HA–GluR1. Cells were treated with or without insulin (0.5 μM, 10 min) and then homogenized as detailed in the Materials and methods section. The expressed AMPA receptor complexes were immunoprecipitated using an anti-HA antibody under denaturing conditions and then immunoblotted for their level of tyrosine phosphorylation using an antiphosphotyrosine antibody. The results demonstrate that there was a detectable level of basal tyrosine phosphorylation of wild-type GluR2 and that the level of phosphorylation increased 39.61 ± 6.94% following brief treatment with insulin (Figure 3C). The triple Y-to-A mutation of HA–GluR2 showed a trend toward decreased basal tyrosine phosphorylation and completely abolished the insulin-induced increase. GluR1 demonstrated very low detectable tyrosine phosphorylation under basal conditions and showed no change after insulin stimulation (Figure 3C). These results suggest that tyrosine phosphorylation of GluR2 CT occurs in a cellular context under basal conditions, and is enhanced by insulin.

The functional significance of GluR2 CT tyrosine phosphorylation with respect to insulin-stimulated endocytosis was tested by assaying internalization of HA–GluR2 and HA–GluR2$_{3Y-3A}$ in HEK293 cells (Figure 4). While mutation of these tyrosine residues did not alter the steady-state level of GluR2 expressed on the cell surface (Figure 4B), it did block the insulin-induced endocytosis (Figure 4A) and insulin-induced reduction in the level of cell-surface AMPA receptors (Figure 4B). These results demonstrate a crucial role for phosphorylation of one or more of these GluR2 CT tyrosine residues in the insulin-dependent AMPA receptor endocytotic pathway.

Native AMPA receptor subunits are differentially tyrosine phosphorylated in adult neurons

To determine whether tyrosine phosphorylation of native GluR2 occurs *in vivo*, cerebral cortex from adult rats was solubilized and immunoprecipitated using an antiphospho-

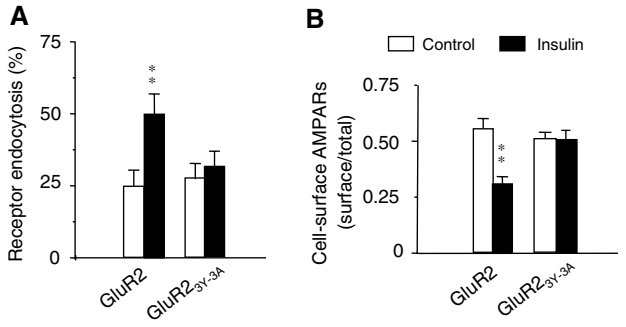

Figure 4 The tyrosine cluster in the GluR2 CT is required for regulated, but not constitutive, AMPA receptor endocytosis in HEK293 cells. (**A**) Colorimetric cell-ELISA receptor endocytosis assays were performed with (insulin) or without (control) stimulation (see Figure 2) on HEK293 cells transiently transfected with wild-type HA–GluR2 subunit or HA–GluR2$_{3Y\text{-}3A}$. (**B**) Colorimetric cell-ELISA cell-surface receptor assay results of HEK293 cells transfected and treated as in (A). Results were obtained from six experiments for each individual group. $^{**}P<0.01$.

tyrosine antibody under both nondenaturing and denaturing conditions. The presence of AMPA receptor subunits in the immunoprecipitates was shown by immunoblotting for GluR2/3 and GluR1 (Figure 5). Under conditions that quantitatively precipitated total tyrosine-phosphorylated proteins (Figure 5, bottom row), a minor but significant fraction of GluR2/3 (on the order of 0.5%) was immunoprecipitated by the antiphosphotyrosine antibody under denaturing conditions (Figure 5, left panel, top row). Under nondenaturing conditions, the same antibody precipitated a larger fraction of GluR2/3, presumably due to multimeric association of non-tyrosine-phosphorylated GluR2/3 with tyrosine-phosphorylated GluR2/3 subunits in the extract (Figure 5, right panel, top row). GluR1 was virtually undetectable in the immunoprecipitates under denaturing conditions, indicating minimal phosphorylation of GluR1 on tyrosines (Figure 5, left panel, second row). The presence of GluR1 in precipitates under nondenaturing conditions (right panel, second row) is presumably due to heteromeric association of GluR1 with tyrosine-phosphorylated GluR2/3. Immunoprecipitation of GluR2/3 by the antiphosphotyrosine antibody was abolished by an excess of phosphotyrosine competitor but not by an excess of phosphoserine, confirming the phosphotyrosine specificity of the immunoprecipitation. By comparison, in the same experiments, NMDA receptor subunit NR2B, but not NR1, was immunoprecipitated by the antiphosphotyrosine antibody under denaturing conditions (Figure 5, left panel, row 3) and the fraction of tyrosine-phosphorylated NR2B is ~10-fold higher than that of GluR2/3. The GluR2/3-binding protein GRIP showed undetectable phosphotyrosine content based on this assay (left panel, row 5). In summary, a small but significant fraction of native GluR2/3, but not GluR1, is tyrosine phosphorylated in the brain under nonstimulated conditions.

Insulin increases tyrosine phosphorylation of GluR2, and depresses AMPA receptor-mediated synaptic transmission in hippocampal slices

We next examined whether insulin stimulation could change the level of tyrosine phosphorylation of AMPA receptors in intact hippocampus. Hippocampal slices were treated with insulin (0.5 μM; 10 min), and GluR1 and GluR2 subunits were then immunoprecipitated under denaturing conditions and immunoblotted with an antiphosphotyrosine antibody (Figure 6). Consistent with the results from cell culture, the GluR2 subunit exhibited a clearly appreciable level of tyrosine phosphorylation under basal conditions; moreover, the level of phosphorylation was increased following insulin stimulation (Figure 6A). In contrast, the tyrosine phosphorylation levels of GluR1 were barely detectable under both

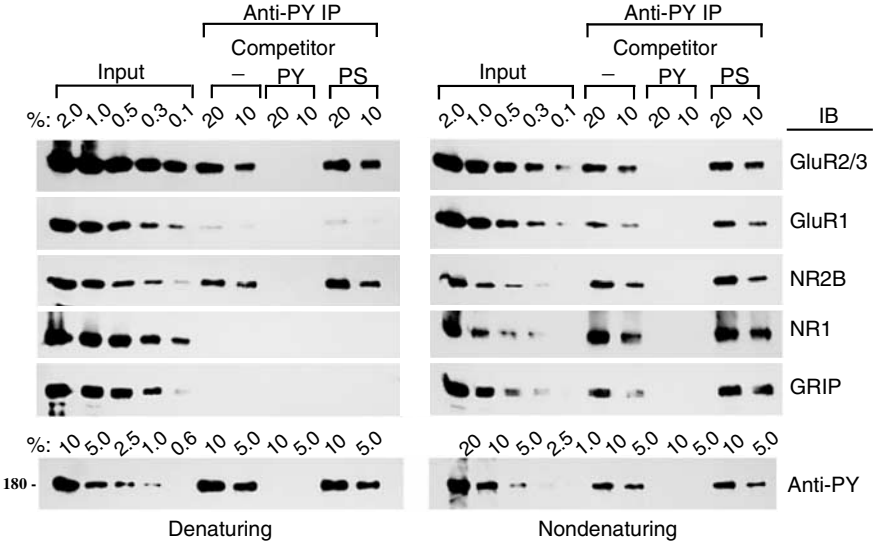

Figure 5 The GluR2 subunit of native AMPA receptors is specifically tyrosine phosphorylated in mature neurons. Membrane proteins from adult rat cerebral cortex were solubilized and immunoprecipitated (IP) using an antiphosphotyrosine antibody (anti-PY; PY20) alone (–) or in the presence of 5 mM phosphotyrosine (PY) or 5 mM phosphoserine (PS) competitor following SDS (denaturing) or DOC (nondenaturing) extraction. The immunoprecipitates were immunoblotted (IB) with antibodies raised against the indicated proteins. Total phosphotyrosine proteins were probed with RC20H to measure the efficiency of precipitation of total phosphotyrosine proteins (bottom row); only the ~180 kDa band is shown. Numbers represent percentage (%) of input (whole lysates) or immunoprecipitate loaded.

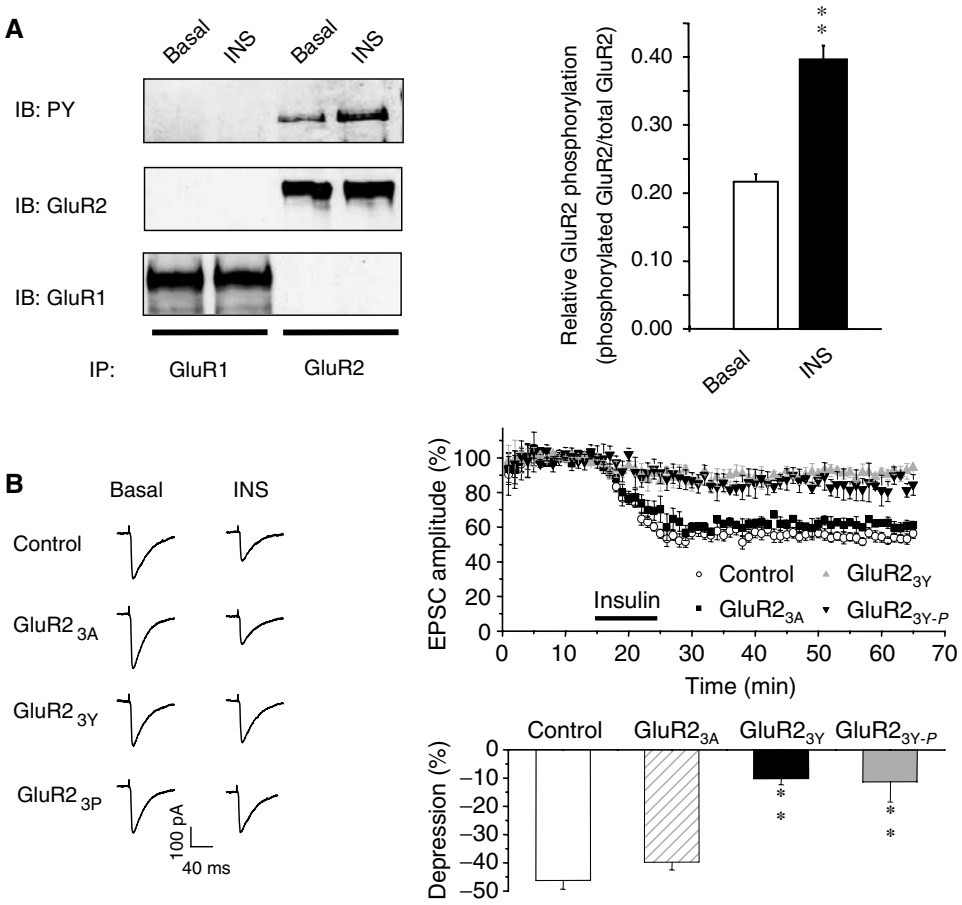

Figure 6 Insulin stimulates tyrosine phosphorylation of GluR2 and long-lasting depression of AMPA receptor-mediated synaptic transmission. (**A**) Tissue homogenates from hippocampal slices treated with (INS) or without (basal) 0.5 μM insulin for 10 min were immunoprecipitated with anti-GluR1 or -GluR2 antibodies under denaturing conditions (IP: GluR1 or GluR2) and immunoblotted using an antiphosphotyrosine antibody (IB: PY). The blot was then sequentially stripped and reprobed with anti-GluR2 (IB: GluR2) or anti-GluR1 (IB: GluR1) antibodies. Densitometric quantitation expressed as the ratio of phosphorylated GluR2 to total GluR2 from three separate experiments is summarized in the histogram on the right. $^{**}P<0.01$. (**B**) EPSCs were recorded in CA1 neurons from hippocampal slices using whole-cell recordings under the voltage-clamp mode at a holding potential of −60 mV. Normalized EPSCs ($EPSC_t/EPSC_5$; the amplitude of EPSCs ($EPSC_5$) is usually stabilized after 5 min of recording) are plotted from neurons recorded with pipettes containing standard intracellular solution (control, $n=7$) or intracellular solution supplemented with $GluR2_{3Y}$ (100 μg/ml; $n=5$), GST–$A_{869}KEGA_{873}NVA_{876}G$ ($GluR2_{3A}$; 100 μg/ml; $n=6$) or the tyrosine-phosphorylated synthetic peptide $Y_pKEGY_pNVY_pG$ ($GluR2_{3Y\text{-}P}$; 50 μg/ml; $n=6$). Time zero is defined as the time point at which the first EPSC was evoked (typically within 1–2 min of the initiation of whole-cell recording). Representative EPSCs averaged from four individual recordings before (basal) or 10 min following application of insulin (INS; 0.5 μM) are shown on the left. Histogram at the bottom right summarizes the depression of the EPSC amplitude after 20 min of insulin stimulation. There was no statistical difference in control versus GST–$GluR2_{3A}$ groups or GST–$GluR2_{3Y}$ versus $GluR2_{3Y\text{-}P}$ ($P>0.5$), but there was a significant difference between control versus GST–$GluR2_{3Y}$ and control versus $GluR2_{3Y\text{-}P}$ ($P<0.001$).

basal and insulin-treated conditions. These results further substantiate the tyrosine phosphorylation of GluR2 in the hippocampus and demonstrate that GluR2 tyrosine phosphorylation can be stimulated by insulin.

To correlate the insulin-stimulated tyrosine phosphorylation with the depression of receptor-mediated excitatory postsynaptic currents (EPSCs) previously observed (Man *et al*, 2000b), we investigated the effect of postsynaptic application of GST–$GluR2_{3Y}$ (GST–YKEGYNVYG), and its mutant counterpart GST–$GluR2_{3A}$ (GST–AKEGANVAG), as a control, during whole-cell recordings of CA1 neurons in hippocampal slices. Neither peptide influenced basal synaptic transmission (data not shown); however, the persistent decrease in the AMPA component of EPSCs normally induced by bath application of insulin was significantly reduced by inclusion of GST–$GluR2_{3Y}$, but not GST–$GluR2_{3A}$ (100 μg/ml), in the recording pipette (Figure 6B). As shown in Figure 3A, GST–$GluR2_{3Y}$, but not GST–$GluR2_{3A}$, is a good tyrosine phosphorylation substrate. These results are consistent with a requirement for tyrosine phosphorylation at these tyrosine residues in insulin-induced EPSC depression. In support of this conjecture, we found that the phosphorylated form of the synthesized peptide Y*p*KEGY*p*NVY*p*G, when included in the recording pipette (50 μg/ml), was also able to decrease significantly the insulin-induced depression of EPSCs (Figure 6B).

Tyrosine residues in the GluR2 CT are critical in mediating LSF-induced LTD

We have previously demonstrated that insulin-induced depression of AMPA EPSCs and low-frequency stimulation (LFS)-induced hippocampal LTD share some common pathways involving clathrin-dependent endocytosis of postsynaptic AMPA receptors (Man *et al*, 2000b). We wondered

whether tyrosine phosphorylation of GluR2 CT might also be required for LFS-induced LTD. First, the level of GluR2 tyrosine phosphorylation was assayed following LFS stimulation of the slices (1 Hz for 15 min, which reliably induces LTD under our experimental conditions; Man *et al*, 2000b). Slices were homogenized in denaturing buffer 10 min after the stimulation, and GluR subunits were immunoprecipitated and probed for phosphotyrosine. As shown in Figure 7A, there was basal tyrosine phosphorylation of GluR2, but not GluR1, and LTD-induced stimulation increased the level of tyrosine phosphorylation of GluR2 without affecting that of GluR1 (Figure 7A). More importantly, the level of LTD produced by LFS was significantly reduced by postsynaptic application of GST–$GluR2_{3Y}$ (100 μg/ml), but not by the mutant peptide GST–$GluR2_{3A}$ (100 μg/ml; Figure 7B). These results suggest that the induction of LTD by LFS requires key tyrosine residues within the GluR2 CT.

Tyrosine residues in the GluR2 CT are critical in mediating insulin-stimulated AMPA receptor endocytosis in neurons

To address directly the roles of GluR2 CT tyrosine residues and their phosphorylation in AMPA receptor endocytosis, we compared AMPA- and insulin-stimulated endocytosis of recombinant AMPA receptors in cultured hippocampal neurons transiently transfected with either wild-type HA–GluR2 or HA–$GluR2_{3Y\text{-}3A}$. At 5 days following transfection, confocal imaging of cell-surface and intracellular receptor expression showed a dramatic reduction in the steady-state cell-surface expression of $GluR2_{3Y\text{-}3A}$ relative to wild type (Figures 8A and B). As demonstrated by 'antibody-feeding'-based receptor endocytosis assays, wild-type HA–GluR2-containing recombinant receptors, like native AMPA receptors (Lin *et al*, 2000; Man *et al*, 2000b), showed a constitutive level of internalization in 10 min that was increased more than two-fold in the presence of either insulin (0.5 μM) or AMPA (100 μM) in the bath medium (Figures 8C and D). However, the 3Y-3A mutations affected both constitutive and stimulated endocytosis. Interestingly, the mutation differentially affected the endocytotic response to insulin and AMPA. HA–$GluR2_{3Y\text{-}3A}$ showed a level of stimulated endocytosis similar to the wild type in response to AMPA (100 μM), but it had little response to insulin (0.5 μM). The results not only provide further evidence supporting a critical role for these tyrosine residues in insulin-stimulated AMPA receptor endocytosis, but further substantiate our previous finding that AMPA- and insulin-stimulated effects on AMPA receptors are mediated by different mechanisms requiring distinct sequences in the GluR2 CT (Lin *et al*, 2000).

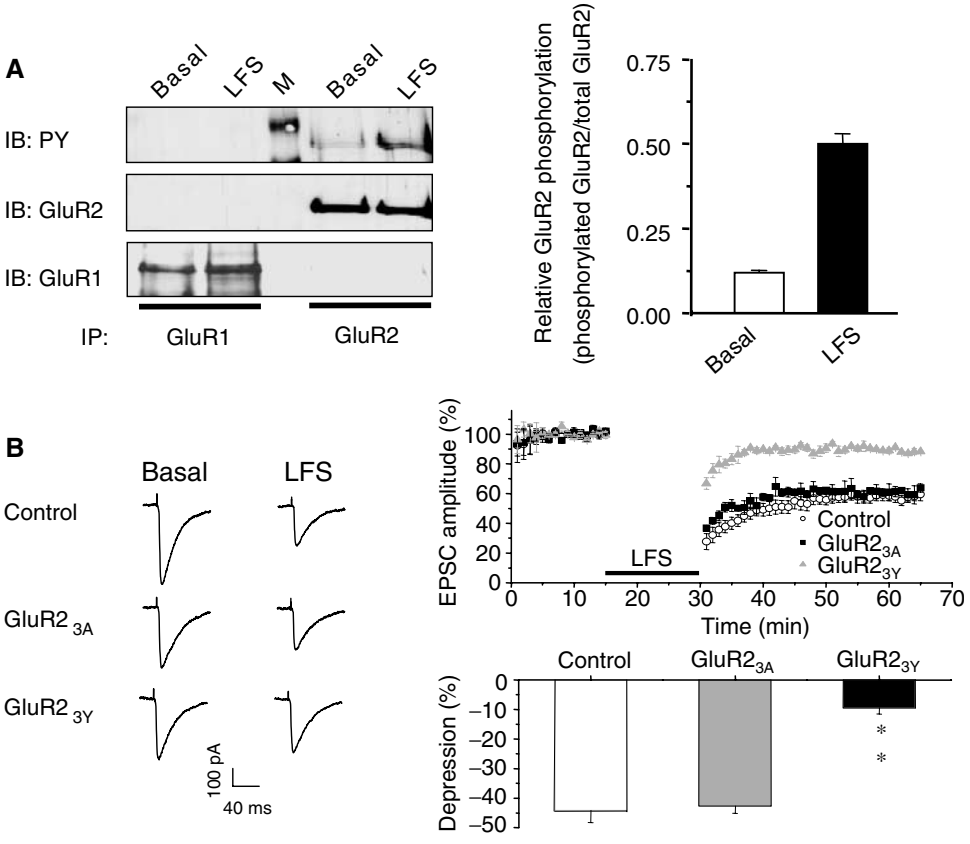

Figure 7 Tyrosine phosphorylation of the GluR2 subunit is required for LFS-induced hippocampal CA1 LTD. (**A**) Homogenates of control or LFS-treated hippocampal slices were immunoprecipitated with anti-GluR1 or GluR2 antibodies and sequentially probed with antiphosphotyrosine (PY), anti-GluR1 (GluR1) and anti-GluR2 antibodies (GluR2) as described for Figure 6. The lane marked M contains molecular weight standards. The results of three individual experiments are summarized in the bar graph. $^{**}P<0.01$. (**B**) Representative responses are shown on the left. The graphs on the right depict normalized EPSCs ($EPSC_t/EPSC_5$) from neurons recorded with pipettes containing standard intracellular solution (control, $n=7$) or intracellular solution supplemented with $GluR2_{3Y}$ ($n=6$) or $GluR2_{3A}$ ($n=7$). The LFS was delivered during the time period indicated by the black horizontal bar. Histogram on the bottom right summarizes the depression of EPSC amplitude 20 min after LFS. The control group was significantly different from the GST–$GluR2_{3Y}$ group ($P<0.001$), but not the GST–$GluR2_{3A}$ group.

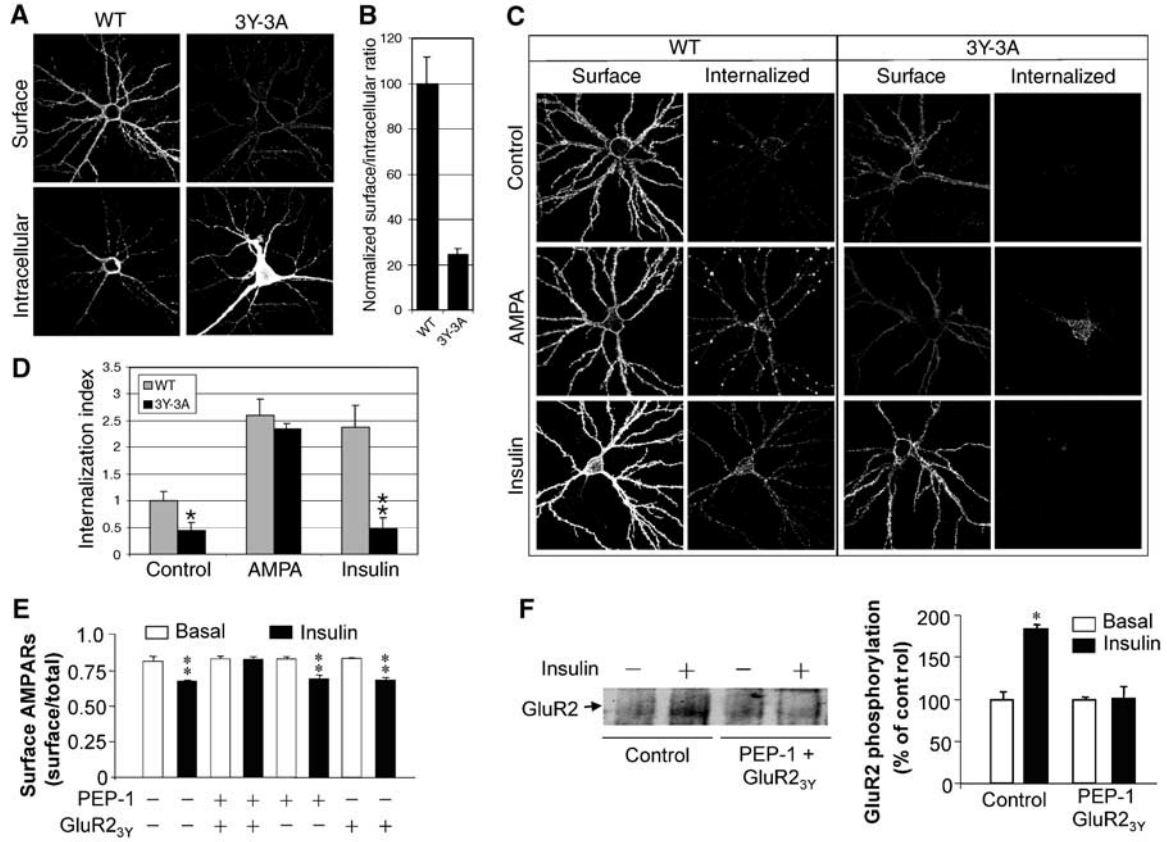

Figure 8 GluR2 CT tyrosine residues are critical for insulin-stimulated endocytosis of AMPA receptors in cultured hippocampal neurons. (**A**) Representative double-label images of surface and intracellular expression of HA–GluR2 wild type (WT) and HA–GluR2$_{3Y\text{-}3A}$ (3Y-3A) in transiently transfected hippocampal neurons. (**B**) Quantitation of surface to intracellular ratio of HA–GluR2$_{3Y\text{-}3A}$, normalized to WT ($n=10$ cells for each construct). (**C**) Representative images of neurons stained for surface and internalized WT and 3Y-3A constructs, after 10 min incubation in either conditioned medium (control), or medium containing 100 μM AMPA (AMPA) or 0.5 μM insulin (insulin). (D) Quantitation of internalization assays, measured as the ratio of internalized to surface fluorescence (internalization index), normalized to WT 10 min control. Histograms show mean ± s.e.m. ($n=8$–10 for each condition). $^{**}P<0.001$ compared with WT plus insulin; $^{*}P<0.05$ compared with WT control. (**E, F**) Cultured hippocampal neurons were treated with (insulin; 0.5 μM) or without (basal) insulin in the presence of either GluR2$_{3Y}$ (1 μM), PEP-1 carrier peptide (20 μM) or both. (E) Cell-surface expression of native AMPA receptors was measured by a colorimetric cell-ELISA assay using an antibody against the N-terminal extracellular domain of native AMPA receptor GluR2 subunits ($n=6$). (F) The level of tyrosine phosphorylation of native AMPA receptor GluR2 was determined by immunoprecipitation of cell lysates with the same anti-GluR2 antibody and immunoblotting with an antiphosphotyrosine antibody (left). Densitometric quantitation expressed as percentage of control is summarized in the histogram on the right ($n=3$). $^{*}P<0.05$.

The altered basal levels of cell-surface expression and constitutive endocytosis in HA–GluR2$_{3Y\text{-}3A}$ transiently expressed in cultured neurons were unexpected since these alterations were not observed when the mutant was expressed in HEK cells (Figure 4) and postsynaptic application of the GluR2$_{3Y}$ peptide did not affect basal synaptic transmission (Figures 6 and 7). The mechanisms responsible for these differences remain unknown, but we suspected that the differences may be in part due to artifacts associated with chronic neuronal overexpression. To explore this further, we examined the effects of a short synthetic GluR2$_{3Y}$ peptide (YKEGYNVYG) on the insulin-stimulated endocytosis of native AMPA receptors in cultured hippocampal neurons using an ELISA cell-surface assay. The peptide (1 μM) was delivered to intracellular compartments by mixing it with a carrier peptide, PEP-1 (Morris *et al*, 2001), for 1 h prior to and during insulin stimulation. As shown in Figure 8E, GluR2$_{3Y}$ in the presence of PEP-1 did not alter the steady-state level of cell-surface expression of AMPA receptors, but prevented any insulin-induced reduction. The blockade of insulin action was also observed when the GluR2$_{3Y}$ peptide, but not the GluR2$_{3A}$ peptide, was delivered into neurons by fusing it to the membrane transduction domain of HIV-1 Tat protein (Supplementary Figure 1). In an attempt to correlate the importance of phosphorylation at these GluR2 CT tyrosine residues in insulin-stimulated endocytosis, we also examined the effect of the GluR2$_{3Y}$ peptide on both basal and insulin-stimulated tyrosine phosphorylation of GluR2 using immunoprecipitation with anti-GluR2 antibody and immunoblotting with antiphosphotyrosine antibody. As shown in Figure 8F, intracellular application of GluR2$_{3Y}$ prevented any insulin-induced increase in the level of tyrosine phosphorylation of GluR2, without altering its basal level of phosphorylation. Consistent with a critical role for tyrosine phosphorylation, we also found that PP2, a specific inhibitor of Src family kinases, prevented the insulin-induced reduction of AMPA receptors (Supplementary Figure 2). These results accord well with the peptide effects on insulin-

stimulated AMPA receptor endocytosis and LTD, suggesting a strong link between insulin-stimulated receptor tyrosine phosphorylation and endocytosis.

Discussion

Recent studies have provided strong evidence that AMPA receptors undergo rapid recycling in the postsynaptic compartment, and therefore the number of receptors on the plasma membrane reflects the balance between exocytotic and endocytotic pathways. AMPA receptors can undergo two modes of endocytosis: constitutive (shown by both GluR1 and GluR2 in the absence of stimulation) and regulated (e.g. following insulin, NMDA or LFS). Insulin- or LFS-induced AMPA receptor internalization is dependent on the GluR2 subunit. We demonstrate in the present study that internal deletion of the membrane proximal 10 amino acids of the GluR2 CT impairs constitutive endocytosis, without altering insulin-stimulated endocytosis and the consequent reduction in receptor levels on the cell surface. On the other hand, truncation of the last 15 amino acids of the CT, or mutation of the three tyrosine residues within this region, blocks insulin-induced endocytosis but has little effect on constitutive endocytosis and basal levels of cell-surface receptor expression. These results clearly demonstrate that constitutive and regulated AMPA receptor endocytotic pathways are mediated by distinct mechanisms that have different sequence requirements.

A short stretch of seven amino acids (EFCYKSR) in the most juxtamembrane region of the CT is 100% conserved among all AMPA receptor GluR subunits. These conserved residues are among the 10 amino acids deleted in $GluR2_{\Delta 834-843}$ and likely contribute to the sequence determinants for constitutive receptor endocytosis, which apply to all GluR subunits. Consistent with this conjecture, we have previously reported that both homomeric GluR1 and GluR2 AMPA receptors are subjected to a similar rate of constitutive endocytosis (Man *et al*, 2000b).

The stretch of 15 amino acids important for insulin-stimulated endocytosis is specific to GluR2 and absent from GluR1, correlating with the endocytotic responsiveness of these subunits to insulin. This sequence contains a cluster of three tyrosine residues ($YKEGYNVY_{876}GIE$), the mutation of which blocks insulin-induced receptor endocytosis and reduction of cell-surface levels. Moreover, we further demonstrated that the GluR2 CT can be tyrosine phosphorylated both *in vitro* and *in vivo*, and that the level of tyrosine phosphorylation of GluR2 is significantly increased following insulin stimulation and dependent on the presence of these three tyrosines. These results suggest that phosphorylation of one or more tyrosine residues within this region is involved in regulated GluR2 endocytosis. The strongest evidence for the requirement of phosphorylation of these tyrosine residues in insulin-stimulated endocytosis comes from the parallel blockades of insulin-stimulated endocytosis and tyrosine phosphorylation of native AMPA receptors in cultured hippocampal neurons by the intracellular application of the $GluR2_{3Y}$ peptide (Figures 8E and F). None of the tyrosine residues conform to any known tyrosine-based internalization sequence motif (Bonifacino and Dell'Angelica, 1999). Thus, how these tyrosines contribute to the regulated internalization of AMPA receptors is unclear. It should also be pointed out that the cluster of three tyrosine residues, although absent from GluR1, are largely conserved among GluR2, GluR3 and GluR4. Thus the signal for insulin-dependent endocytosis might be present in most of the AMPA receptor subunits and confer regulation on the majority of native heteromeric AMPA receptors that contain GluR2, GluR3 or GluR4.

Several lines of evidence suggest that tyrosine phosphorylation of this GluR2 tyrosine-containing internalization signal may be important in the control of the strength of AMPA receptor-mediated synaptic transmission and thereby play an indispensable role in the expression of certain forms of synaptic plasticity. First, the GluR2, but not the GluR1, subunit of native AMPA receptors in the rat cortex and hippocampus is tyrosine phosphorylated. More importantly, the level of GluR2 tyrosine phosphorylation is rapidly increased by insulin stimulation in association with a long-lasting depression of AMPA receptor-mediated EPSCs. The blockade of this insulin-induced long-lasting depression by postsynaptic injection of either $GluR2_{3Y}$ or $GluR2_{3Y\text{-}P}$, but not by the mutant $GluR2_{3A}$, supports the involvement of GluR2 tyrosine phosphorylation in the insulin-induced EPSC depression. Second, LFS induction of hippocampal CA1 LTD is associated with increased GluR2 tyrosine phosphorylation, and is prevented by GST–$GluR2_{3Y}$ but not the control peptide GST–$GluR2_{3A}$. Third, Boxall *et al* (1996) have reported evidence that tyrosine phosphorylation is also required for the expression of a cerebellar LTD, the expression of which has been shown to require a GluR2 CT-dependent AMPA receptor endocytosis (Wang and Linden, 2000; Xia *et al*, 2000). Perhaps the most convincing evidence, as mentioned above, is the blockade of both insulin-stimulated GluR2 tyrosine phosphorylation and AMPA receptor endocytosis by acute intracellular application of $GluR2_{3Y}$ peptide in cultured hippocampal neurons (Figures 8E and F). Admittedly, while we have provided strong evidence supporting a role for GluR2 tyrosine phosphorylation, we still cannot rule out the possible involvement of other tyrosine phosphorylation targets in the control of AMPA receptor trafficking, thereby contributing to the expression of certain forms of LTD.

The tyrosine kinase(s) that phosphorylates the GluR2 CT remains to be identified. The blockade of insulin-induced AMPA receptor endocytosis by PP2 (Supplementary Figure 2) suggests the involvement of a nonreceptor Src family kinase in the action of insulin. Postsynaptic injection of the insulin receptor neutralizing antibody, while blocking insulin-induced depression of AMPA EPSCs, had little effect on either hippocampal homosynaptic LTD (LD Liu and YT Wang, unpublished data) or cerebellar LTD (Wang and Linden, 2000), indicating that a tyrosine kinase, other than the insulin receptor itself, may be required for the expression of these forms of LTD. In this regard, it is relevant to note that an Src family kinase has previously been shown to be required for cerebellar LTD (Boxall *et al*, 1996). Thus, activation of an Src kinase may represent a convergent point by which both insulin and LFS stimulate GluR2 phosphorylation. In the present study, we primarily use insulin as a tool to study the molecular mechanisms underlying the regulated endocytosis of AMPA receptors and its role in the expression of hippocampal homosynaptic LTD. It should however be noted that, although insulin is not required for expression of electric stimulation-induced LTD in both hippocampal slices and

cerebellar cultures, insulin may have important roles in mediating certain other forms of synaptic plasticity in humans and animals since insulin receptors are found to be concentrated in the postsynaptic density of neurons (Abbott *et al*, 1999) and neurons are able to release insulin in an activity-dependent manner (Wozniak *et al*, 1993).

In addition to this tyrosine-rich sequence of GluR2, there may be other domains or sequences that are also critical for the regulated AMPA receptor endocytosis. One domain that has recently been implicated is the PDZ domain (S_{880}KVI) in the extreme GluR2 CT. Several recent studies have provided strong evidence that disrupting PDZ domain-mediated protein interactions, the GluR2–PICK1 interaction in particular, impairs regulated AMPA receptor endocytosis (Chung *et al*, 2000) and prevents the expression of hippocampal and cerebellar LTD (Xia *et al*, 2000; Kim *et al*, 2001; but see also Daw *et al*, 2000). Thus, although the exact underlying mechanisms remain to be determined, the SKVI sequence in the GluR2 CT may be another internalization signal involved in regulated AMPA receptor endocytosis. Given the fact that interfering with either the tyrosine-containing region (the present work) or the SKVI signal (Xia *et al*, 2000; Kim *et al*, 2001) could block AMPA receptor endocytosis and LTD production in neurons, both signals are functional and may be indispensably involved in regulated AMPA receptor endocytosis in neurons. The mechanisms by which these multiple internalization signals act in concert during various forms of synaptic plasticity remain to be illustrated.

Thus, in addition to constitutive endocytosis, AMPA receptors have been shown to be subjected to stimulated endocytosis by diverse stimuli including growth factors, such as insulin/IGF-1 (the present work) (Man *et al*, 2000b; Wang and Linden, 2000), agonist binding (Beattie *et al*, 2000; Ehlers, 2000; Lin *et al*, 2000) and LTD-producing protocols (Luscher *et al*, 1999; Man *et al*, 2000b; Wang and Linden, 2000). It is therefore very likely that there exist different, stimulus-dependent mechanisms that contribute to different forms of synaptic plasticity.

Materials and methods

cDNA plasmids and cell transfection

Rat HA-tagged GluR1 and GluR2 receptor subunit cDNAs have been described previously (Man *et al*, 2000b). Other constructs of HA–GluR2 were made using PCR methods or the Quick-Change Site Directed Mutagenesis Kit (Stratagene) as detailed in Supplementary data. HEK293 cells (ATCC) were transfected using the calcium phosphate precipitation method. At 36–48 h after transfection, cells were washed with extracellular recording solution (ECS in mM: 140 NaCl, 33 glucose, 25 HEPES, 5.4 KCl, 1.3 $CaCl_2$; pH 7.4, 320 mOsm) and incubated in ECS for at least 1 h (serum starvation). For insulin treatment, cells were incubated with ECS supplemented with (treatment) or without (control) 0.5 μM human recombinant insulin (Sigma) for 10 min. Cells were washed and incubated for an additional 20 min in ECS without supplementation. The cells were then processed for immunocytochemistry or colorimetric assays, or lysed in RIPA buffer (50 mM Tris–HCl, 150 mM NaCl and 0.1% Triton X-100) for immunoprecipitation as described below.

Cloning, expression and purification of GST fusion proteins

GST–$GluR2_{3Y}$ and GST–$GluR2_{3A}$ were constructed by subcloning corresponding PCR fragments into pGEX 4T-1 vectors. GST fusion proteins were expressed in DH5α *Escherichia coli* and purified from bacterial lysates according to the manufacturer's protocol (Pharmacia). Products were dialyzed in PBS and concentrated using Microcon-10 columns (Amicon) for intracellular application during whole-cell recordings.

Immunofluorescent confocal microscopy

HEK293 cells were plated onto poly-D-lysine-coated glass coverslips set in 35 mm culture dishes and transfected with 2 μg of the plasmid of interest. For cell-surface receptor expression assays, cells at 48 h post-transfection were fixed with 4% paraformaldehyde in PBS for 10 min. Surface AMPA receptors were first labeled with monoclonal anti-HA antibody (1:2000, Babco, Berkeley, CA) and visualized with an FITC-conjugated anti-mouse IgG antibody (1:500, Sigma). For the surface AMPA receptor internalization assay, HEK293 cells transfected with HA-tagged GluR2 constructs were incubated live at 4°C with monoclonal anti-HA antibody (10 μg/ml) for 1 h to label surface AMPA receptors. Cells were then incubated at 37°C in ECS supplemented with or without 0.5 μM insulin for 10 min followed by a wash and additional 20 min incubation in fresh ECS (without supplementation) to allow for constitutive or regulated internalization of labeled receptors. Following a 10 min fixation with 4% paraformaldehyde without permeabilization, receptors remaining on the plasma membrane surface were stained with FITC-conjugated anti-mouse IgG antibodies. The internalized cell-surface receptors were subsequently labeled with Cy3-conjugated anti-mouse IgG antibodies following cell permeabilization as described by Man *et al* (2000b).

Colorimetric assays

Colorimetric assays were performed essentially as previously reported (Man *et al*, 2000b) and detailed in Supplementary data.

Immunoprecipitation and Western blotting

Immunoprecipitation and Western blotting were carried out essentially as previously reported (Man *et al*, 2000b). Proteins from cerebral cortex, hippocampal slices, cultured hippocampal neurons or transfected HEK293 cells were solubilized in RIPA buffer containing either 1% SDS (plus 5 min boiling; denaturing conditions) or 1% DOC (nondenaturing conditions). For immunoprecipitation, 500 μg of protein from these tissue lysates was incubated with their respective antibodies in 500 μl of RIPA buffer for 4 h at 4°C. Protein A–sepharose was added to the mixture and incubated for an additional 2 h. The complex was isolated by centrifugation and washed three times. Proteins eluted from the sepharose beads were subjected to SDS–PAGE and immunoblotting using their respective antibodies. For sequential reprobing of the same blots, the membranes were stripped of the initial primary and secondary antibodies and subjected to immunoblotting with another antibody. Blots were developed using enhanced chemiluminescence detection (Amersham). Band intensities were quantified using Scion Image PC software.

Hippocampal neuron cultures, transfection and fluorescence-based internalization assays

These have recently been published (Passafaro *et al*, 2001; Lee *et al*, 2002) and are briefly described in Supplementary data.

Electrophysiological recording

Whole-cell recordings of CA1 EPSCs from hippocampal slices prepared from Sprague–Dawley rats aged 16–26 postnatal days were performed essentially as previously described (Man *et al*, 2000b) and detailed in Supplementary data.

Statistical analysis

Student's *t*-tests were used whenever intra-experiment samples were compared. For crosscomparisons or analysis of data between experiments, all values were first subjected to a one-way ANOVA and all groups were compared against control basal values. Values were not statistically significant at $F > 0.5$. Groups that were found to be statistically significant were individually compared using Dunnett's *t*-test. For normalized (%) data comparison, data were analyzed using a nonparametric statistical test (Kolmogorov–Smirnov test).

Supplementary data

Supplementary data are available at *The EMBO Journal* Online.

Acknowledgements

This work was supported by grants-in-aid from the Heart and Stroke Foundation of BC and Yukon (NA-3762), Canadian Institutes of Health Research and the EJLB Foundation to YTW, and the NIH to MS (NS35050). MS is an Associate Investigator of the Howard Hughes Medical Institute. YTW is a Howard Hughes Medical Institute International Scholar and the holder of the Heart and Stroke Foundation of BC and Yukon Chair in Stroke Research at the University of British Columbia and Vancouver Hospital & Health Sciences Centre.

References

Abbott MA, Wells DG, Fallon JR (1999) The insulin receptor tyrosine kinase substrate p58/53 and the insulin receptor are components of CNS synapses. *J Neurosci* **19:** 7300–7308

Beattie EC, Carroll RC, Yu X, Morishita W, Yasuda H, von Zastrow M, Malenka RC (2000) Regulation of AMPA receptor endocytosis by a signaling mechanism shared with LTD. *Nat Neurosci* **3:** 1291–1300

Bonifacino JS, Dell'Angelica EC (1999) Molecular bases for the recognition of tyrosine-based sorting signals. *J Cell Biol* **145:** 923–926

Boxall AR, Lancaster B, Garthwaite J (1996) Tyrosine kinase is required for long-term depression in the cerebellum. *Neuron* **16:** 805–813

Carroll RC, Beattie EC, Xia H, scher C, Altschuler Y, Nicoll RA, Malenka RC, von Zastrow M (1999) Dynamin-dependent endocytosis of ionotropic glutamate receptors. *Proc Natl Acad Sci USA* **96:** 14112–14117

Chung HJ, Xia J, Scannevin RH, Zhang X, Huganir RL (2000) Phosphorylation of the AMPA receptor subunit GluR2 differentially regulates its interaction with PDZ domain-containing proteins. *J Neurosci* **20:** 7258–7267

Daw MI, Chittajallu R, Bortolotto ZA, Dev KK, Duprat F, Henley JM, Collingridge GL, Isaac JT (2000) PDZ proteins interacting with C-terminal GluR2/3 are involved in a PKC-dependent regulation of AMPA receptors at hippocampal synapses. *Neuron* **28:** 873–886

Duprat F, Daw M, Lim W, Collingridge G, Isaac J (2003) GluR2 protein–protein interactions and the regulation of AMPA receptors during synaptic plasticity. *Philos Trans R Soc Lond B* **358:** 715–720

Ehlers MD (2000) Reinsertion or degradation of AMPA receptors determined by activity-dependent endocytic sorting. *Neuron* **28:** 511–525

Hayashi Y, Shi SH, Esteban JA, Piccini A, Poncer JC, Malinow R (2000) Driving AMPA receptors into synapses by LTP and CaMKII: requirement for GluR1 and PDZ domain interaction. *Science* **287:** 2262–2267

Hollmann M, Heinemann S (1994) Cloned glutamate receptors. *Annu Rev Neurosci* **17:** 31–108

Kim CH, Chung HJ, Lee HK, Huganir RL (2001) Interaction of the AMPA receptor subunit GluR2/3 with PDZ domains regulates hippocampal long-term depression. *Proc Natl Acad Sci USA* **98:** 11725–11730

Lee SH, Liu L, Wang YT, Sheng M (2002) Clathrin adaptor AP2 and NSF interact with overlapping sites of GluR2 and play distinct roles in AMPA receptor trafficking and hippocampal LTD. *Neuron* **36:** 661–674

Liang F, Huganir RL (2001) Coupling of agonist-induced AMPA receptor internalization with receptor recycling. *J Neurochem* **77:** 1626–1631

Lin JW, Ju W, Foster K, Lee SH, Ahmadian G, Wyszynski M, Wang YT, Sheng M (2000) Distinct molecular mechanisms and divergent endocytotic pathways of AMPA receptor internalization. *Nat Neurosci* **3:** 1282–1290

Lu W, Man H, Ju W, Trimble WS, MacDonald JF, Wang YT (2001) Activation of synaptic NMDA receptors induces membrane insertion of new AMPA receptors and LTP in cultured hippocampal neurons. *Neuron* **29:** 243–254

Luscher C, Xia H, Beattie EC, Carroll RC, von Zastrow M, Malenka RC, Nicoll RA (1999) Role of AMPA receptor cycling in synaptic transmission and plasticity. *Neuron* **24:** 649–658

Luthi A, Chittajallu R, Duprat F, Palmer MJ, Benke TA, Kidd FL, Henley JM, Isaac JT, Collingridge GL (1999) Hippocampal LTD expression involves a pool of AMPARs regulated by the NSF–GluR2 interaction. *Neuron* **24:** 389–399

Man HY, Ju W, Ahmadian G, Wang YT (2000a) Intracellular trafficking of AMPA receptors in synaptic plasticity. *Cell Mol Life Sci* **57:** 1526–1534

Man HY, Lin JW, Ju WH, Ahmadian G, Liu L, Becker LE, Sheng M, Wang YT (2000b) Regulation of AMPA receptor-mediated synaptic transmission by clathrin-dependent receptor internalization. *Neuron* **25:** 649–662

Matsuda S, Launey T, Mikawa S, Hirai H (2000) Disruption of AMPA receptor GluR2 clusters following long-term depression induction in cerebellar Purkinje neurons. *EMBO J* **19:** 2765–2774

Morris MC, Depollier J, Mery J, Heitz F, Divita G (2001) A peptide carrier for the delivery of biologically active proteins into mammalian cells. *Nat Biotechnol* **19:** 1173–1176

Passafaro M, Piech V, Sheng M (2001) Subunit-specific temporal and spatial patterns of AMPA receptor exocytosis in hippocampal neurons. *Nat Neurosci* **4:** 917–926

Pickard L, Noel J, Duckworth JK, Fitzjohn SM, Henley JM, Collingridge GL, Molnar E (2001) Transient synaptic activation of NMDA receptors leads to the insertion of native AMPA receptors at hippocampal neuronal plasma membranes. *Neuropharmacology* **41:** 700–713

Wang YT, Linden DJ (2000) Expression of cerebellar long-term depression requires postsynaptic clathrin-mediated endocytosis. *Neuron* **25:** 635–647

Wenthold RJ, Petralia RS, Blahos J, II, Niedzielski AS (1996) Evidence for multiple AMPA receptor complexes in hippocampal CA1/CA2 neurons. *J Neurosci* **16:** 1982–1989

Wozniak M, Rydzewski B, Baker SP, Raizada MK (1993) The cellular and physiological actions of insulin in the central nervous system. *Neurochem Int* **22:** 1–10

Xia J, Chung HJ, Wihler C, Huganir RL, Linden DJ (2000) Cerebellar long-term depression requires PKC-regulated interactions between GluR2/3 and PDZ domain-containing proteins. *Neuron* **28:** 499–510

